

DIFFERENT ASPECTS OF SEED LAYER-PRINTED AND LIGHT-INDUCED PLATED FRONT SIDE CONTACTS

M. Hörteis, J. Bartsch, V. Radtke, A. Filipovic, S. W. Glunz

Fraunhofer Institute for Solar Energy Systems, Heidenhofstr. 2, D-79110 Freiburg, Germany

Phone +49-761-4588-5493; Fax +49-761-4588-9287,

email: matthias.hoerteis@ise.fraunhofer.de

ABSTRACT:

The properties of fine-line printed contacts on silicon solar cells, in combination with light-induced plating (LIP), are investigated. The seed layers are printed using an aerosol system and a new metallization ink called *SISC* developed at Fraunhofer ISE. The influence of multiple layer printing on the contact geometry is studied as well as the influence of the contact height on the line resistivity and on the contact resistance. As the line resistivity of fine-line printed fingers needs to be reduced by LIP, three different plating electrolytes are tested on solar cells. The observed differences in line resistivity between $\rho_f = 5 \times 10^{-8} \Omega\text{m}$ and $2 \times 10^{-8} \Omega\text{m}$ are explained by taking SEM pictures of the grown LIP silver. Finally, the optimum LIP height for different line resistivities is calculated and experimentally confirmed by processing solar cells with an increasing amount of LIP silver.

KEYWORDS: metallization, fine line printing, light-induced plating

1. INTRODUCTION

The metallization of silicon solar cells is playing an increasingly important role in order to produce silicon solar cells more cost-effectively. An improved front side metallization helps to reach this goal by increasing the cell efficiency and by reducing the material costs. For this, several two-layer methods and materials have been investigated at ISE over the past few years [1, 2]. For deposition of the first, the contact layer, two promising approaches were successfully tested at ISE and efficiencies of more than 20% could be achieved: (i) a low-temperature processes where nickel is electroless deposited [3] directly on the emitter - the SiN_x coating is previously opened [4] - and a metal silicide is formed at moderate temperatures of $T < 400^\circ\text{C}$. (ii) a high-temperature process where the contact metal is aerosol printed [5] on the anti reflection coating and fired through at temperatures above 700°C .

The emphasis of this work is on the plated layer, which is responsible for the current transport. One very promising way to create a high-conductive contact is light-induced plating (LIP) [6]. For lab-type solar cells cyanidic electrolytes for light-induced plating has been used at Fraunhofer ISE since 1992 [7]. Due to its reliability and low lateral finger resistivity ($\rho_f = 1.9 \times 10^{-8} \Omega\text{m}$), it is considered as a kind of reference process for all industrially feasible, non-toxic, in-line plating solutions of which two have been analyzed in detail.

2 EXPERIMENT

Initially, a seed layer with a negligible influence on the plated silver was deposited. Therefore we aerosol-printed [8] fine seed layers on industrially large-area multicrystalline silicon solar cells and co-fired them in an in-line belt furnace. To investigate the influence of the electrolyte on the conductivity of the contact finger three different electrolytes were used to thicken the seed layer in a LIP process [6]. One of them was a cyanidic electrolyte (CN-LIP) and two were non-cyanidic (NCN1 and NCN2). The contact fingers were isolated by a dicing saw and the influence of the plating solution on the line

conductivity was determined by a 4-probe measurement before and after an annealing step. Additionally, the contact micro-structure was analyzed by SEM images.

Further on, ten multicrystalline solar cells of a size of $15.6 \text{ cm} \times 15.6 \text{ cm}$ were contacted with a seed layer grid. The cells were divided in two groups of 5 cells. Each group was successively plated and consecutively IV-measured in order to determine the optimum amount of LIP-silver for two plating solutions (CN and NCN1).

3. SIMULATION

The two-layer concept is only advantageous compared to a single layer (e.g. a thick screen printed) contact, if the plated silver has a high conductivity. In Figure 1, the total losses (electrically and optically) are simulated as a function of the plated silver height and width, respectively for different resistivities. A simulation [9] was performed for an infinitely thin and $30 \mu\text{m}$ wide layer with a resistivity of $\rho_c = 1 \text{ m}\Omega\text{cm}^2$ on an emitter with a sheet resistance of $R_{SH} = 60 \Omega/\text{sq}$. For the width of the total contact a growth mechanism of 1:2 (height:width) was assumed. The simulated grid has 80 fingers and 3 bus bars (1.5 mm each) on a $15.6 \text{ cm} \times 15.6 \text{ cm}$ large mc-Si solar cell.

At small plating heights, the loss p_{tot} is dominated by electrical losses and strongly dependent on the amount of deposited silver. At large plating heights the loss mechanism is dominated by optical losses, due to an increased finger width. The total loss curve is not symmetric, i.e. the dependence of the total loss is higher for smaller finger heights. Thus, concerning the total cell loss, it is more favourable to plate too much silver than too little. The solar cell efficiency is very stable over a broad range of plated silver mass, see below. A high specific conductivity of the plated silver is beneficial in two ways: The total losses were diminished and the amount of required silver is smaller and the required process time for plating is shorter. For example, if the line resistivity is reduced from $\rho_f = 3 \times 10^{-8} \Omega\text{m}$ to $\rho_f = 1.9 \times 10^{-8} \Omega\text{m}$ the optimum line height can be reduced from $14 \mu\text{m}$ to $11 \mu\text{m}$ (21%) the line width by 10% and the cross section from $730 \mu\text{m}^2$ to $520 \mu\text{m}^2$. As the cross

section is nearly directly proportional to the amount of plated silver, 28% less silver is consumed.

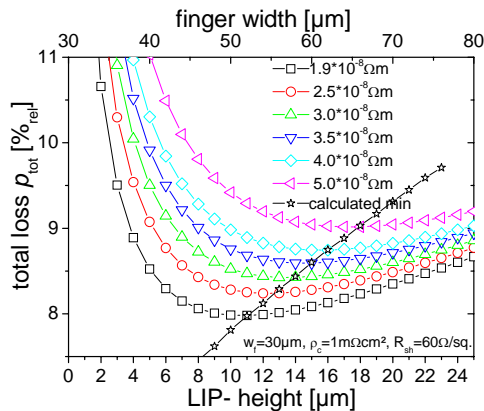


Figure 1: Simulation of the total losses (optical and electrical) dependent on the amount (height) of deposited silver for different line resistivities.

4. LINE RESISTIVITY AND MICROSTRUCTURE

The line resistivity of aerosol-printed and subsequent light-induced plated fingers is shown in Figure 2. The aerosol printed seed layer is thin enough ($<1 \mu\text{m}$) and its contribution to the resistivity is negligible as the plated silver has a height of $15 \mu\text{m}$ and more. The plating parameter like light intensity, applied potential, pH-value and temperate which were kept in an optimized range for each electrolyte [10]. Thus the growth mechanism and the morphology are determined by the used electrolyte. The strong influence of the used electrolyte on the line resistivity can be explained by SEM-images, see Figure 3. Also the influence of an annealing step becomes clear. Both, the macroscopic shape of the plated finger and the microcrystallinity are influenced by the different electrolytes: The silver layer deposited from the NCN1-electrolyte shows a botryoidally morphology. The several clusters can reach the size of the height of the finger, thus, more than $10 \mu\text{m}$ in diameter. The clusters, although very fine grained, can be distinguished. As the resistivity is determined by the smallest cross section, the current flow is mainly limited by these deep incisions. For the measurement of the resistivity we determined an average cross section and the botryoidal structure is levelled. Supposed that the resistivity of a single cluster is high and in the range of bulk silver, due to the rough morphology and the cluster boundaries, the line resistivity is limited, even if the contact losses across the cluster boundaries can be reduced by an annealing. Thus, a large fraction of plated silver does not contribute to the current flow.

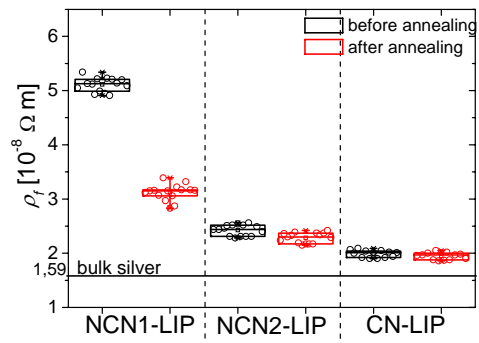


Figure 2: Line resistivity ρ_f for three different plating solutions, before and after an annealing step of 10 min at $T=350^\circ\text{C}$.

In case of the NCN2-solution, the several Ag-clusters are pyramidal or trigonal to a certain extent. They are much smaller, below $1 \mu\text{m}$ and deep incisions which would reduce the cross section and the measured resistivity are not visible. The LIP-silver grows homogeneously at the surface at the ratio of 1:2 (height:width) resulting in a roundish shaped contact. The surface roughness is determined by the small Ag-clusters and almost all the plated silver contributes to the current flow. The measured resistivity of $\rho_f=2.2 \times 10^{-8} \Omega\text{m}$ can only slightly be improved by an annealing step, indicating the dense silver deposition and the excellent conductivity between the single Ag-grains.

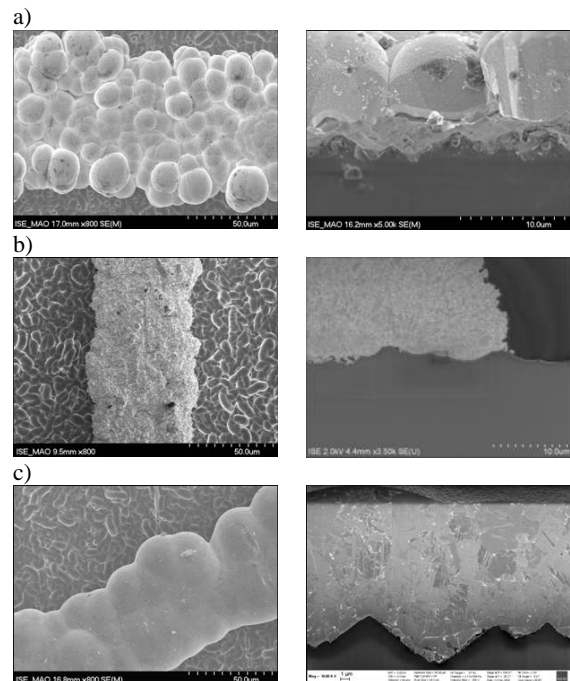


Figure 3: SEM-image of the plated, conductive layer: a) For a non-cyanidic (NCN1) plating solution. Noticeable are the large cluster boundaries and the botryoidally growth. b) For a non-cyanidic (NCN2) plating solution and c) for a cyanidic (CN) plating solution the surfaces are much smoother and the individual grains are less distinct.

The best values for line resistivity can be achieved with the cyanidic electrolyte. The measured average value of $\rho_l=1.9 \times 10^{-8} \Omega\text{m}$ is close to the resistivity of bulk silver ($\rho_l=1.59 \times 10^{-8} \Omega\text{m}$). The surface is smooth, i.e. no Ag-clusters can be distinguished any more. Possibly, the structure reveals single Ag-grains in a SEM-image of a polished cross section. The grain boundaries between the grains are hardly visible, and an influence of an annealing step on the resistivity is barely measurable. However, further investigations have to be performed to reveal the correlation between layer structure (on different scales) and electrical properties.

In conclusion, the cyanidic plating solution is the best choice in terms of electrical and optical properties. Also the process stability is much higher for cyanidic electrolytes. However the healthy risks in an industrial production have to be taken into account. A good alternative to the cyanidic electrolyte is the plating solution NCN2 which results in a line resistivity close to the one of cyanidic plating. .

5 SOLAR CELL RESULTS

15.6 cm x 15.6 cm mc-solar cells with a seed layer grid with 80 fingers and 2 bus bars, aerosol-printed and fired were used to perform an experiment concerning the cell fill factor (FF) as well as the series resistance (R_s) in dependence on the mass of LIP-silver, see Figure 4. Examined were the LIP-solutions CN and NCN1, respectively. A continuous increase of the FF with the mass of plated silver $Ag\text{-LIP}$ was observed together with a steady decrease of R_s . In case of the CN solution the FF reached its saturation at a silver mass of approximately 100 mg per wafer whereas similar FF s were reached for the NCN1 solution at about 130 mg. The line resistance is continuously reduced with the quantity of deposited LIP silver and both, the values for R_s and for the FF are improving. Exceeding a LIP-silver mass of about 200 mg, an improvement for both electrolytes was hardly measurable and the FF s were constant in the tested range.

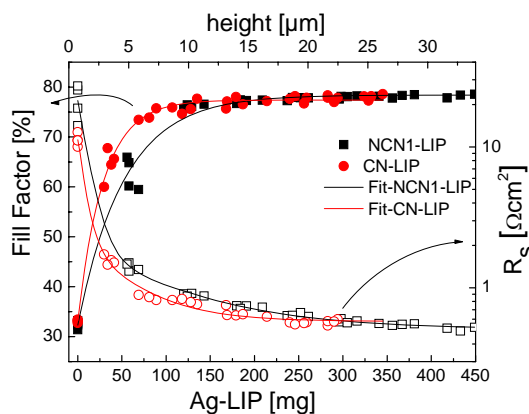


Figure 4: Fill factor (FF) and series resistance (R_s) as a function of the mass of plated silver ($Ag\text{-LIP}$) for both, NCN and CN plating solutions.

The short-circuit current density (j_{sc}) is quite sensitive to the mass of plated silver and decreases linearly with the deposited silver amount, see Figure 5. For both plating-

solutions a slope of about $-1.6 \text{ (mA/cm}^2\text{)}/100\text{mg}$ was observed. From the measured current densities, j_{sc_ini} (after short LIP) and j_{sc_LIP} (after LIP) an effective finger width (w_{eff}) can be calculated. If the non-metallized active cell area after seed layer deposition is known (A_{active_ini}), the actual non-metallized area (A_{active_eff}) and the according *optically effective* metallized area for the plated grid fingers (A_{fi_eff}) for all values of j_{sc} can be determined and transferred into an effective finger width. It is well known that the optical effective width of a contact finger can be considerably smaller than its geometrical width [11, 12].

$$w_{eff} = \frac{A_{fi_eff}}{l_{fi} \times n_{fi}},$$

$$\text{with } A_{fi_eff} = A_{tot_cell} - A_{active_eff} - A_{BB}$$

$$\text{and } A_{active_eff} = \frac{j_{sc_LIP}}{j_{sc_ini}} \times A_{active_ini}$$

Eq. 1: Calculation of the effective contact width, determined from the j_{sc} values where l_{fi} is the finger length, n_{fi} is the total number of fingers, A_{BB} is the total area of the busbars.

The calculated *optically effective* finger width for the NCN1-LIP is shown. The *geometrical* finger width w_f , determined from a microscopic picture, for a contact plated with 360 mg NCN1-LIP is about $w_f=100 \mu\text{m}$. Its effective width, determined from the current density, is about $w_{eff}=87 \mu\text{m}$. This reduction will be even higher if the cells are encapsulated into a module due to the internal reflection at the glass-air interface [12].

The effective width for CN-LIP contact is even smaller and the average j_{sc} -values for the CN-LIP are about 0.2 mA/cm^2 above the average current density of the NCN1-LIP even if they are built up with the same amount of LIP-silver. The 0.2 mA higher j_{sc} values in case of CN-LIP can be translated into a reduction in effective contact width by $10 \mu\text{m}$ which gives in total an absolute increase in the cell efficiency of $\Delta\eta=0.1\%$.

The cell efficiency reaches its maximum at about 200 mg for both solutions. Passing this point, the gain in efficiency due to an increasing FF is compensated by the steady decrease in j_{sc} . The cell efficiency is constant over a broad range and starts to decrease due to the growing shading losses at LIP quantities of 350 mg for CN-LIP and 450 mg for NCN1-LIP, respectively. As expected from the simulation, the cell efficiency is quite invariant with respect to high quantities of LIP silver.

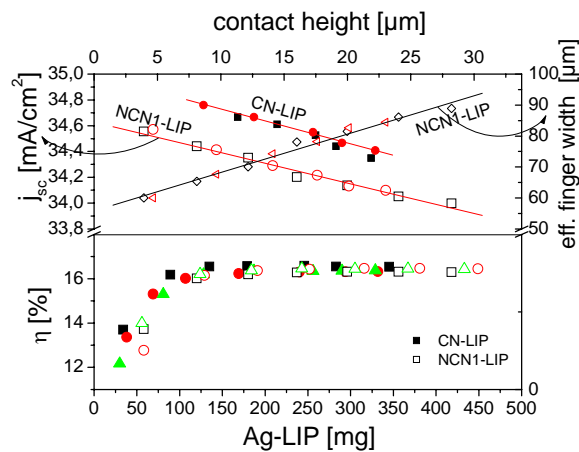


Figure 5: Current density j_{sc} and cell efficiency η as a function of LIP silver mass and contact height from the constant decrease in j_{sc} , an effective finger width is calculated

6 SUMMARY

The electrical performance of fine-line printed seed layers, subsequently plated were studied in detail on test samples and on solar cells. Regarding the electrical properties of a two-layer contact it is beneficial to both, the line resistivity and the contact resistance to keep the seed layer as thin as possible. The fraction of the seed layer of the total contact cross section needs to be minimized while the fraction of the LIP silver should be maximized to achieve lowest values for the line resistivity of about $\rho_f=1.9 \times 10^{-8} \Omega m$. Additionally, the influence of the height of the printed seed layer on the contact resistance was investigated. The contact formation between the seed layer and the emitter of a solar cell is more efficient for a thin ($h < 2 \mu m$) than for a thick ($h = 2-9 \mu m$) seed layer. In SEM images the influence of the seed layer thickness on the contact interface was investigated. For a low contact resistance it is important to etch as little material from the wafer (SiN_x -layer, Si) to keep the resulting glass layer as thin as possible. For a good front side metallization the printed line height of the seed layer should be as low as possible, just enough to form a low ohmic contact, to achieve a good adhesion and to provide a good ability for plating. As the specific line resistivity of the total contact is determined by the quality of the deposited LIP-silver, different plating solutions were investigated by analyzing the plated contacts. Different line resistivities, from close to bulk silver (CN-LIP) up to resistivities comparable to screen printed contacts (NCN1-LIP) were found. The optimum mass of LIP-silver necessary to metalize a solar cell is determined theoretically and experimentally. A line resistivity of $\rho_f=1.9 \times 10^{-8} \Omega m$ compared to $\rho_f=3.0 \times 10^{-8} \Omega m$ saves almost 30% of silver. In addition, measuring the current of solar cells as a function of plated silver, the effective optical finger width is determined to be about 15% smaller than the geometrical contact width as the current density of a standard solar cell, is reduced by 1.6 mA/cm² per 100 mg plated silver.

ACKNOWLEDGEMENT

The authors gratefully would like to thank all members from ISE who contributed to this work especially Daniel Schmidt for solar cell printing, Johannes Spannagel for resistance- and TLM measurements, Damian Pysch for his support in grid simulation and Elisabeth Schäffer for measuring the cell parameters.

REFERENCES

1. Glunz, S.W., et al. "Progress in advanced metallization technology at Fraunhofer ISE", *Proc. 33rd IEEE PVSC*. 2008. San Diego, USA.
2. Glunz, S.W., et al. "New concepts for the front side metallization of silicon solar cells", *Proc. 21st EU PVSEC*. 2006. Dresden, Germany.
3. Alemán, M., et al. "Advances in electroless nickel plating for the metallization of silicon solar cells using different structuring techniques for the ARC ", *proc. 24th EU-PVSEC*. 2009. Hamburg, Germany.
4. Knorz, A., et al. "Laser ablation of antireflection coatings for plated contacts yielding solar cell efficiencies above 20 %", *proc. 24th EU-PVSEC*. 2009. Hamburg, Germany.
5. Hörteis, M. and S.W. Glunz "Fine line printed silicon solar cells exceeding 20% efficiency", *Progr. Photovolt.*, 16 2008, pp. 555-60.
6. Mette, A., et al. "Increasing the efficiency of screen-printed silicon solar cells by light-induced silver plating", *Proc. 4th WCPEC*. 2006. Waikoloa, Hawaii, USA.
7. Glunz, S.W., et al. "Comparison of different dielectric passivation layers for application in industrially feasible high-efficiency crystalline silicon solar cells", *Proc. 20th EC PVSEC* 2005. Barcelona, Spain.
8. Mette, A., et al., "Metal aerosol jet printing for solar cell metallization", *Progr. Photovolt.*, 115 2007, pp. 621-7.
9. Mette, A., New concepts for front side metallization of industrial silicon solar cells, in *Fakultät für Angewandte Wissenschaften*. 2007, Universität Freiburg: Freiburg, p. 231.
10. Bartsch, J., et al. "Progress in understanding the current paths and deposition mechanisms of light-induced plating and implication for the process", *EU-PVSEC* 2009. Hamburg.
11. Blakers, A.W., "Shading losses of solar-cell metal grids", *J. Appl. Phys.*, 71 1992, pp. 5237-41.
12. Woehl, R., M. Hörteis, and S.W. Glunz "Analysis of the optical properties of screen-printed and aerosol-printed and plated fingers of silicon solar cells", *Advances in OptoElectronics*, 2008 2008.